

# Chaotic advection in point vortex models and two-dimensional turbulence

A. Babiano

Laboratoire de Meteorologie Dynamique, ENS, 24 Rue Lhomond, Paris Cedex 05, France

G. Boffetta

Istituto di Fisica Generale, Università di Torino, Via P. Giuria 1, I-10126 Torino, Italy

A. Provenzale

Istituto di Cosmogeofisica del CNR, Corso Fiume 4, I-10133 Torino, Italy

A. Vulpiani

Dipartimento di Fisica, Università di Roma "La Sapienza," Piazzale Aldo Moro 2, I-00185 Roma, Italy

(Received 18 May 1993; accepted 17 March 1994)

The dynamics of passively advected particles in either integrable or chaotic point vortex systems and in two-dimensional (2-D) turbulence is studied. For point vortices, it is shown that the regular or chaotic nature of the particle trajectories is not determined by the Eulerian chaoticity of the vortex motion, but rather by pure Lagrangian quantities, such as the distance of an advected particle from the vortex centers. In fact, each point vortex turns out to be surrounded by a regular island, where the advected particles are trapped and their Lagrangian Lyapunov exponent is zero, even though the vortex itself may perform a chaotic trajectory. In the field between the vortices, passive particles undergo chaotic advection with an associated positive Lyapunov exponent. For well-separated vortices, even at large times, the advected particles do not cross the boundary between the chaotic sea and the regular islands surrounding the vortices. A similar situation holds in the case of forced-dissipative 2-D turbulence, where particles trapped in the interior of the coherent structures have a null Lagrangian Lyapunov exponent, while those in the background turbulent sea move chaotically. This gives clear evidence of the important role played by chaotic advection, even in complex Eulerian flows.

## I. INTRODUCTION

Understanding the dynamics of passive tracers in laminar and turbulent flows has important implications on both applied and fundamental research. In past years, this subject has been intensively studied by using several different methods. The classic viewpoint, based on the concepts of turbulent diffusion,<sup>1</sup> has been recently complemented by the approach based on dynamical system theory; this latter theory has led to the discovery of chaotic advection and of the phenomenon of tracer dispersion in simple laminar Eulerian flows; see, e.g., Refs. 2–5 for recent reviews. In the present paper, we consider the problem of chaotic advection in a system of point vortices and in two-dimensional (2-D) turbulence. The goal of the work is to determine whether and how the concepts of chaotic advection may be used to study Eulerian flows with complex time evolution, as well as to understand the effects of coherent structures on the particle motion. A physical motivation for this work may be found, e.g., in the discussion given in Ref. 3.

We remark that it is highly nontrivial to extract information on the Lagrangian properties (e.g., diffusion and mixing), starting from an Eulerian point of view. For instance, there are situations where the velocity field is regular—i.e., absence of Eulerian chaos—but the corresponding motion of fluid particles is chaotic; see, e.g., Refs. 6–14 for some examples of particle advection studies in given time-dependent Eulerian flows. On the other hand, it has been shown that a chaotic Eulerian velocity field may generate a regular Lagrangian behavior, in the sense that two fluid particles initially very close do not separate at an exponential rate.<sup>14</sup> The

above properties make it rather problematic to infer the “true” nature of the Eulerian velocity field, starting from Lagrangian observations. For this reason, it is important to know the effects of the most common Eulerian structures on particle advection; in particular, the role of coherent vortices should be carefully evaluated.

The equations of motion of a fluid particle initially located at  $\mathbf{x}(0)$  in the Eulerian velocity field  $\mathbf{u}(\mathbf{x},t)$  are given by

$$\frac{d\mathbf{x}}{dt} = \mathbf{u}(\mathbf{x},t), \quad (1)$$

with the initial condition  $\mathbf{x}(0)$ . For a two-dimensional incompressible fluid (i.e.,  $\nabla \cdot \mathbf{u} = 0$ ) Eq. (1) assumes the Hamiltonian form [ $\mathbf{x} = (x, y)$  and  $\mathbf{u} = (u, v)$ ]:

$$\frac{dx}{dt} = \frac{\partial \psi}{\partial y}, \quad \frac{dy}{dt} = -\frac{\partial \psi}{\partial x}, \quad (2)$$

where the Hamiltonian  $\psi$  is the streamfunction related to the velocity field by

$$u = \frac{\partial \psi}{\partial y}, \quad v = -\frac{\partial \psi}{\partial x}. \quad (3)$$

Equations (1) or (2) also define the motion of test particles, such as powder grains embedded in the fluid, under the condition that the particles are small enough not to perturb the velocity field, but also large enough not to perform a Brownian motion. Particles of this type are the tracers used for flow visualization in fluid mechanics experiments. In the present paper, we consider only the case of tracers with the same density of the fluid; the more general case of impurities

with density different from the fluid has been treated, e.g., in Refs. 15 and 16 for particularly simple choices of the streamfunction.

A first observation concerns the difference between Eulerian and Lagrangian chaos. The former indicates the chaotic behavior (in the sense of sensitive dependence on initial conditions) of the equations governing the time evolution of the velocity field. Conversely, the term Lagrangian chaos indicates the sensitive dependence on initial conditions of the solutions of Eq. (1) in a given velocity field. In general, a quantitative measure of the degree of chaoticity is given by the value of the largest *Lyapunov exponent*; see, e.g., Refs. 17 and 18 for introductions to chaotic dynamics. The presence of Lagrangian chaos, even in the absence of Eulerian chaos, indicates that some gross properties of mixing and diffusion are not strongly related to the presence of Eulerian turbulence. An intriguing issue considered here is to understand whether the properties of particle dynamics in 2-D turbulence are necessarily related to the presence of Eulerian turbulence or they are due just to the phenomenon of Lagrangian chaos as found even in simple models of chaotic advection.

The remainder of this paper is organized as follows.

In Sec. II we discuss the chaoticity of passive particle trajectories in the regular and chaotic velocity fields generated by the motion of three and four point vortices. We find that the presence of Lagrangian chaos is not related to the regular or chaotic nature of the Eulerian flow, but rather to the distance of the advected particles from a vortex center (that is, by a purely Lagrangian condition).

In Sec. III we consider the motion of an ensemble of advected particles in the same velocity fields considered above, and we discuss the properties of the regular islands surrounding the moving vortices.

In Sec. IV we study the chaoticity of particle trajectories in a numerical simulation of forced-dissipative 2-D turbulence and we compare the results with those obtained for point vortices.

Summary and conclusions are given in Sec. V, together with some general comments on the relationships between Eulerian and Lagrangian properties.

## II. ADVECTION IN POINT VORTEX MODELS

In this section we consider the motion of passively advected particles in the velocity field generated by three or four point vortices in the infinite domain. The dynamics of systems of point vortices has been thoroughly studied since the pioneering work of Kirchhoff;<sup>19</sup> see, e.g., Ref. 20 for a review. The motion of a system of  $N$  point vortices with vorticities  $\Gamma_1, \Gamma_2, \dots, \Gamma_N$  and positions  $[x_i(t), y_i(t)]$ ,  $i = 1, \dots, N$ , is described by the Hamiltonian system,

$$\Gamma_i \frac{dx_i}{dt} = \frac{\partial H}{\partial y_i}, \quad (4a)$$

$$\Gamma_i \frac{dy_i}{dt} = -\frac{\partial H}{\partial x_i}, \quad (4b)$$

where

$$H = -\frac{1}{4\pi} \sum_{i \neq j} \Gamma_i \Gamma_j \ln r_{ij}, \quad (5)$$

and  $r_{ij}^2 = (x_i - x_j)^2 + (y_i - y_j)^2$ . In the case of point vortices on the torus or on the sphere, it is sufficient to substitute the  $\ln r_{ij}$  in Eq. (5) with the appropriate Green's function  $G(r_{ij})$ ; see, e.g., Ref. 21.

In general, the motion of  $N$  point vortices may be described in an Eulerian phase space with  $2N$  dimensions. A system of three vortices with arbitrary values of  $\Gamma_i$  is integrable;<sup>20</sup> the vortex motion is in this case regular (i.e., there is no exponential divergence of nearby trajectories in phase space). For  $N \geq 4$ , apart nongeneric initial conditions and/or values of the parameters  $\Gamma_i$ , the system appears, in general, to be chaotic.<sup>20,22</sup> In the following, we study the motion of a passively advected particle located in  $[x(t), y(t)]$  in the velocity field defined by Eqs. (4) and (5), by numerically integrating the equations (1), which in the present case, become

$$\frac{dx}{dt} = -\sum_i \frac{\Gamma_i}{2\pi} \frac{y - y_i}{R_i^2}, \quad (6a)$$

$$\frac{dy}{dt} = \sum_i \frac{\Gamma_i}{2\pi} \frac{x - x_i}{R_i^2}, \quad (6b)$$

where  $R_i^2 = (x - x_i)^2 + (y - y_i)^2$ . A similar problem has been considered in Ref. 23. In the following, for the point vortex system we use the natural time and space units, which are fixed by the values of the parameters  $\Gamma_i$ . Note that the Lagrangian phase space of the passive particle motion has two dimensions ( $x$  and  $y$ ); the total phase space of the system of  $N$  vortices plus the advected particle has thus  $2N + 2$  dimensions.

First let us consider the motion of advected particles in a three-vortex (integrable) system. In this case, the streamfunction for the advected particle is periodic in time and the expectation is that the advected particles may display chaotic behavior. Here we have chosen  $\Gamma_1 = \Gamma_2 = \Gamma_3 = 10$ . The motion of the vortices and of the advected particles has been computed by a fourth-order Runge-Kutta integrator with time step  $\Delta t = 5 \times 10^{-3}$ . Figures 1(a) and 1(b) show two typical trajectories of passive particles that have initially been placed, respectively, in close proximity of a vortex center or in the background field between the vortices. The two trajectories display very different behavior. The particle seeded close to the vortex center displays a regular oscillatory motion around the moving vortex; by contrast, the particle in the background field undergoes an irregular and aperiodic trajectory.

In order to provide a quantitative confirmation of the above observation, we have calculated the maximum Lyapunov exponent of the Lagrangian motion (6) for both cases. Given two infinitesimally close trajectories  $\mathbf{x}(t)$  and  $\mathbf{x}(t) + \epsilon \mathbf{z}(t)$ , solutions to (1), in the limit  $\epsilon \rightarrow 0$  the time evolution of the separation vector  $\mathbf{z}(t)$  is given by the linearized equation:

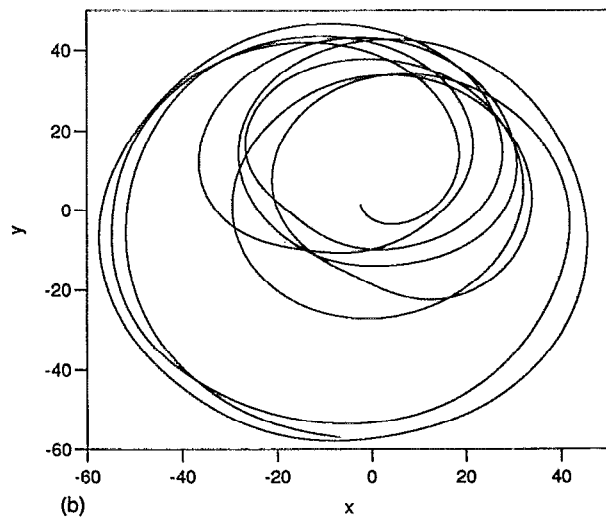
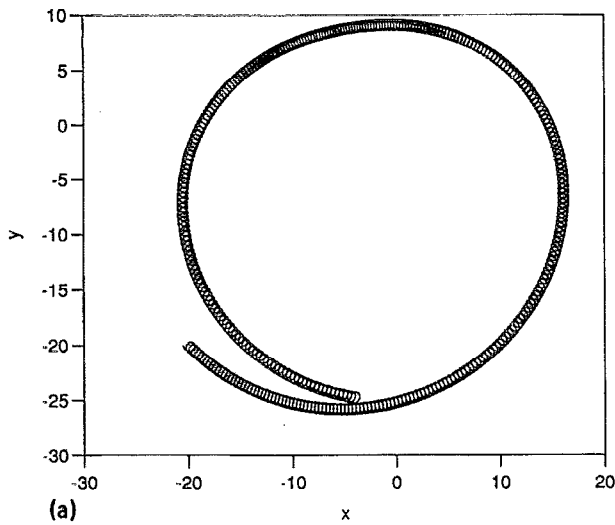


FIG. 1. Particle trajectories in the three-vortex system. The Eulerian dynamics is, in this case, integrable ( $\lambda_E=0$ ). Panel (a) shows a regular trajectory and panel (b) shows a chaotic Lagrangian trajectory. The different behavior of the two particles is due to different initial conditions.

$$\frac{dz}{dt} = \frac{\partial \mathbf{u}}{\partial \mathbf{x}} \mathbf{z}, \quad (7)$$

where  $\partial \mathbf{u} / \partial \mathbf{x}$  is the Jacobian with components  $\partial u_i / \partial x_j$ ,  $i, j = 1, 2$ . The maximum Lagrangian Lyapunov exponent  $\lambda_L$  is then defined as

$$\lambda_L = \lim_{t \rightarrow \infty} \Lambda_L(t) = \lim_{t \rightarrow \infty} \frac{1}{t} \ln \frac{|\mathbf{z}(t)|}{|\mathbf{z}(0)|}. \quad (8)$$

For a Hamiltonian system such as (2), a regular, predictable Lagrangian behavior is associated with  $\lambda_L=0$ , while chaotic Lagrangian dynamics and unpredictable particle trajectories are associated with a value  $\lambda_L > 0$ .

The practical evaluation of  $\lambda_L$  may be obtained by two different numerical algorithms, either by the direct implementation of (7) and (8), see Ref. 24, or by the method of Benettin *et al.*,<sup>25</sup> which is based on integrating the motion of two nearby particles (a “true” particle and a “ghost” particle), and on periodically replacing the ghost particle with

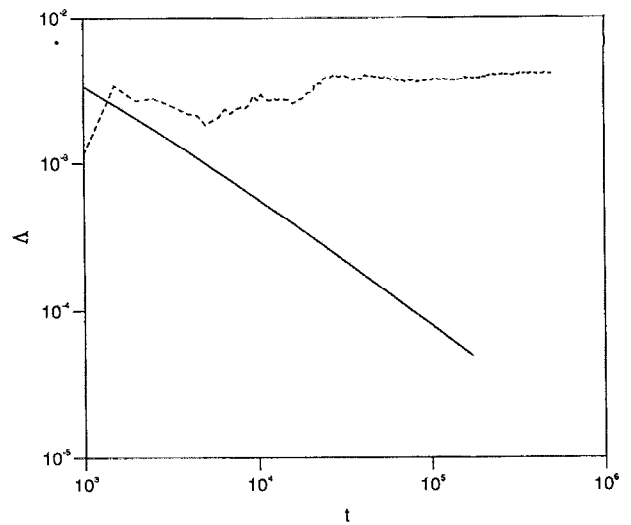


FIG. 2. Values of the quantity  $\Lambda_L(t)$  for the two trajectories shown in Fig. 1. The solid curve is for the trajectory in Fig. 1(a) and the dashed curve is for the particle path in Fig. 1(b). The Lagrangian Lyapunov exponents are obtained as limits of  $\Lambda_L(t)$  for  $t \rightarrow \infty$ .

another one close to the real particle. In fact, both methods require a periodic normalization of the solution of (7), either for avoiding growth of  $e\mathbf{z}(t)$  beyond the linear perturbation regime with the ghost particle method or to avoid numerical overflows due to the exponential increase of  $|\mathbf{z}(t)|$  when the Jacobian method is used. To this end, following Ref. 24, we integrate (7) on a period  $T$ , starting with a normalized vector  $\mathbf{z}(0)$  [ $|\mathbf{z}(0)|=1$ ], and then compute the quantity

$$d(T) = \frac{1}{T} \ln |\mathbf{z}(T)|. \quad (9)$$

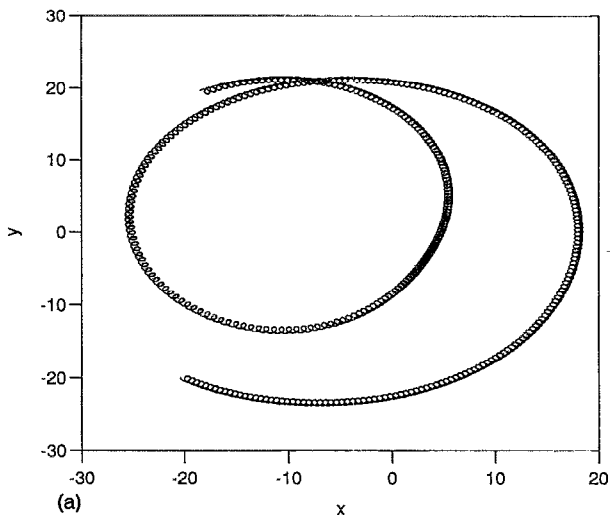
The vector  $\mathbf{z}(T)$  is then normalized (being careful not to change its orientation) and the integration is performed on another period  $T$ . By repeating this procedure  $n$  times, the original definition of the Lyapunov exponent is then recovered through

$$\lambda_L = \lim_{n \rightarrow \infty} \frac{1}{n} \sum_{k=1}^n d_k(T), \quad (10)$$

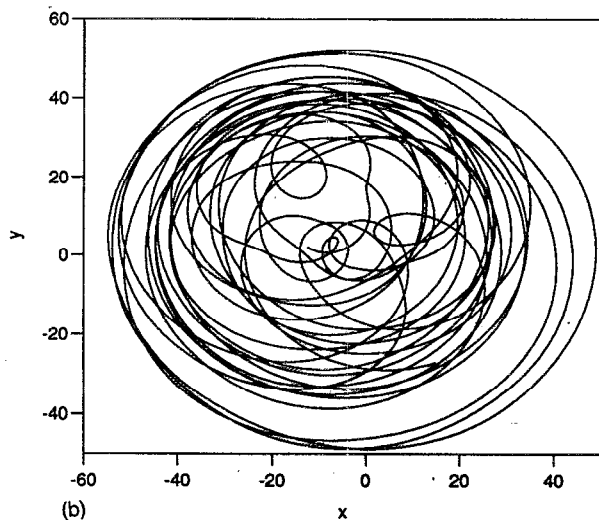
where  $d_k(T)$  indicates the quantity given by Eq. (9) in the  $k$ th period of duration  $T$ .

Figure 2 reports the quantity  $\Lambda_L(t)$  vs  $t$  for the two trajectories shown in Fig. 1. The exponent  $\Lambda_L$  converges to zero for the particle close to the vortex center, indicating the non-chaotic nature of the particle motion. Conversely,  $\Lambda_L(t)$  converges to a well-defined positive value  $\lambda_L$  for the particle in the background field between the vortices, confirming the chaotic nature of the Lagrangian motion when the advected particle is sufficiently far from the vortices.

The Eulerian Lyapunov exponent  $\lambda_E$  is defined in a similar way by considering the exponential divergence of two solutions of (4) in the  $2N$ -dimensional phase space of the motion of the  $N$  vortices, i.e.,



(a)



(b)

FIG. 3. Particle trajectories in the four-vortex system. The Eulerian dynamics is in this case chaotic. Panel (a) shows a regular Lagrangian trajectory and panel (b) shows a chaotic Lagrangian trajectory. The different behavior of the two particles is due to different initial conditions.

$$\lambda_E = \lim_{t \rightarrow \infty} \Lambda_E(t) = \lim_{t \rightarrow \infty} \frac{1}{t} \ln \frac{|\zeta(t)|}{|\zeta(0)|}, \quad (11)$$

where  $\zeta(t) = [\zeta_1(t), \dots, \zeta_{2N}(t)]$  evolves, according to the linearization of (4),

$$\frac{d\zeta}{dt} = \frac{\partial \mathbf{F}}{\partial \mathbf{p}} \zeta, \quad (12)$$

where  $\mathbf{p}$  is the phase-space coordinate of the vortex system and  $\mathbf{F}$  is the right-hand side of Eq. (4). Note that for both particle trajectories shown in Fig. 1, we have considered the same vortex dynamics, which is integrable, i.e., nonchaotic, with  $\lambda_E = 0$ .

The above results confirm that the Lagrangian particle trajectories may be chaotic, even for a regular Eulerian flow. We now consider a case where the Eulerian flow is chaotic. To this end it is sufficient to consider a system [(4) and (5)] with  $N \geq 4$ . Figures 3(a) and 3(b) report the trajectories of two passive particles deployed, respectively, in proximity of

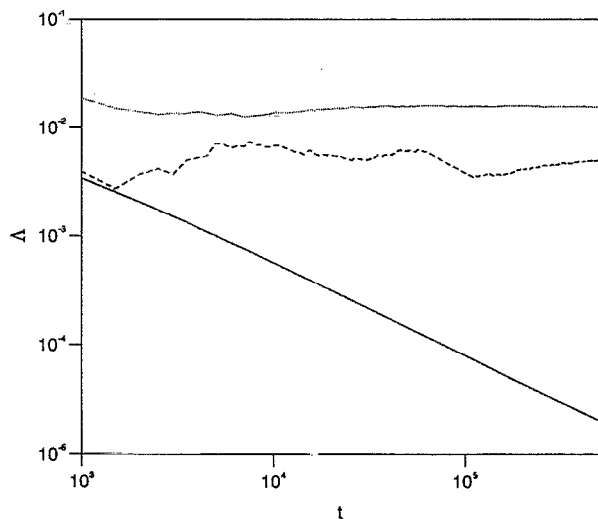


FIG. 4. Values of the quantity  $\Lambda_L(t)$  for the two trajectories shown in Fig. 3. The solid curve is for the trajectory in Fig. 3(a) and the dashed curve is for the particle path in Fig. 3(b). The dotted curve shows the quantity  $\Lambda_E(t)$  for the Eulerian dynamics. The Lagrangian or Eulerian Lyapunov exponents are obtained as limits of  $\Lambda(t)$  for  $t \rightarrow \infty$ .

a vortex center and in the background field between the vortices, for  $N=4$  and  $\Gamma_1 = \Gamma_2 = \Gamma_3 = \Gamma_4 = 10$ . In the first case, the particle rotates around the moving vortex. The vortex motion is chaotic; consequently, the particle position is unpredictable on large times, as is the vortex position. Nevertheless, the Lagrangian Lyapunov exponent for this trajectory converges to zero, as shown in Fig. 4. Note that in this case the Eulerian Lyapunov exponent is positive, as shown in Fig. 4 as well.

The regular motion of the advected particle around an irregularly moving center is not in contradiction with its zero Lagrangian Lyapunov exponent, as the positive Eulerian Lyapunov exponent refers to the vortex motion and the null Lagrangian Lyapunov exponent implies that two nearby particles remain close during their motion, performing a regular orbit around the chaotically moving vortex. A similar behavior has been observed in the case of the Lorenz model.<sup>14</sup> The present results indicate that the existence of regular regions of Lagrangian motion, even in chaotic (or turbulent, see Sec. IV) Eulerian flows may be a general property of particle advection processes.

Analogous to what has been observed for the three-vortex system, also for  $N=4$ , there are chaotic particle trajectories [see Fig. 3(b) and the corresponding Lagrangian Lyapunov exponent shown in Fig. 4]. These results indicate once more that there is no strict link between Eulerian and Lagrangian chaoticity. In the present situation, the discriminator between regular and chaotic behavior is the distance of the advected particles from the vortices. In general, we note that there is no particle ejection from the regular islands for (numerically) arbitrarily large integration times. This behavior suggests a true asymptotic nature of the regular islands, whose radius is determined by the minimum distance between the vortex under consideration and the nearest hyperbolic point (in a system of  $N$ -point vortices on the infinite plane, there are  $N-1$  hyperbolic points). The relationship

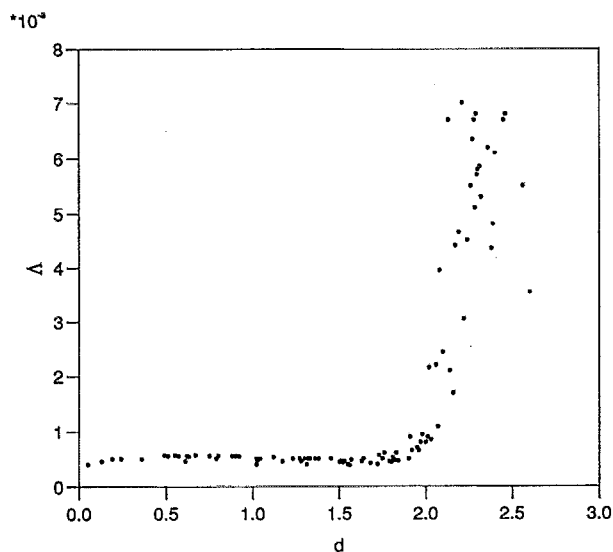


FIG. 5. Values of  $\Lambda_L(t_{fin})$  versus the initial particle distance from the closest vortex, for 100 particles seeded at random in the four-vortex system. The quantity  $t_{fin}=20\,000$  is the total simulation time for this experiment. For distances smaller than an empirically determined threshold value  $d_c \approx 2$ , the motion is regular, while for larger values of  $d_c$  the Lagrangian motion is chaotic.

between the minimum distance of the nearest hyperbolic point and the size of the regular island has been directly verified for the system of three-point vortices, and it will be discussed in a forthcoming paper. *A posteriori*, the above results seem to be qualitatively analogous to the existence of invariant curves separating regular and chaotic regions in nonintegrable Hamiltonian systems. The difference of the present case relies upon the fact that the Hamiltonian is not time periodic, and the size, position, and shape of the regular islands may aperiodically vary with time.

In order to further characterize the coexistence of regular and chaotic Lagrangian behavior in vortex systems, we have evaluated the Lagrangian Lyapunov exponents for an ensemble of 100 initial conditions chosen at random in the vortex domain. The trajectories appear to be roughly divided in two classes: The regular trajectories where  $\Lambda_L(t) \rightarrow 0$  and the chaotic ones where  $\Lambda_L(t) \rightarrow \lambda_L > 0$ . In Fig. 5 we show the value of  $\Lambda_L(t_{fin})$  at the maximum simulation time  $t_{fin}=20\,000$  versus the initial distance  $d$  of each particle from the closest vortex. The particle motion is regular up to a threshold distance  $d_c$ , as indicated by the very small value of  $\Lambda_L(t_{fin})$  for  $d \leq d_c$ . For initial distances larger than  $d_c$ , the particles move in the chaotic region, and the Lagrangian Lyapunov exponent has a finite positive value. This behavior confirms the presence, around each vortex, of a region of regular Lagrangian motion. Note that  $\Lambda_L(t_{fin})$  cannot be strictly equal to zero in the regular regions due to the finite simulation time. The regular nature of the Lagrangian motion in this case is indicated by the fact that for these particles  $\Lambda_L(t)$  decreases as a power law and that  $\Lambda_L(t_{fin})$  is comparable with  $1/t_{fin}$ .

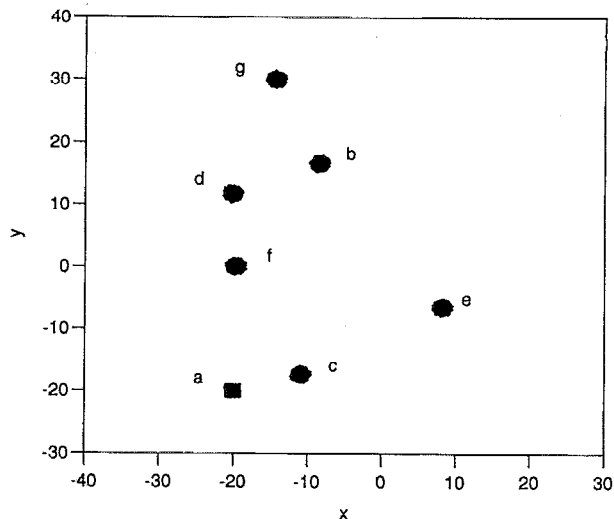


FIG. 6. Positions of 1000 Lagrangian particles initially seeded in proximity of a vortex for the four-vortex system, at different instants of time. The labels *a–g* refer to the times  $t=0, 500, 1000, 1500, 2000, 2500,$  and  $3000$  natural time units. The initial distribution is the square cloud centered in  $(-20, -20)$ . The particles do not escape from the regular island surrounding the (irregularly moving) vortex.

### III. SPREADING OF AN ENSEMBLE OF ADVECTED PARTICLES

The chaotic or regular nature of the trajectories (in the sense of a positive or null value of  $\lambda_L$ ) determines the dispersive or “compact” nature of clouds of particles advected by the Eulerian field. In fact, in the case  $\lambda_L=0$  there is no divergence of nearby particles and absent or slow spreading of the particle clouds, even though the center of mass of the cloud may perform an irregular trajectory in the presence of a chaotic Eulerian velocity field. Conversely, in the case

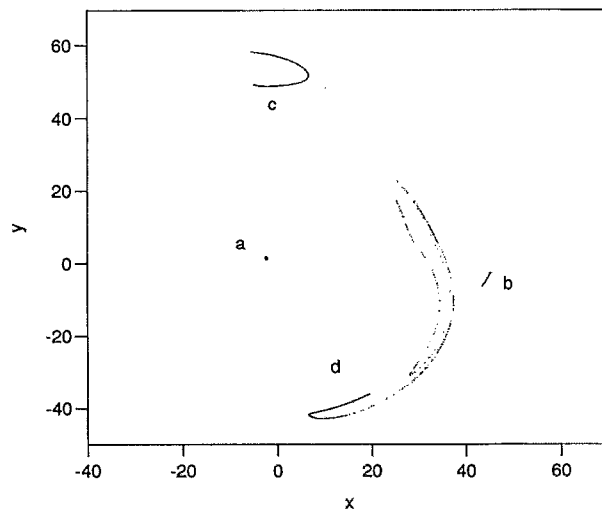


FIG. 7. Positions of 10 000 Lagrangian particles initially seeded in the background chaotic sea between the vortices for the four-vortex system, at different instants of time. The labels *a–d* refer to the times  $t=0, 500, 1000,$  and  $1500$  natural time units. The initial distribution is the small square cloud centered in  $(0, 2)$ . The particle distribution undergoes stirring and folding as usually observed for chaotic systems.

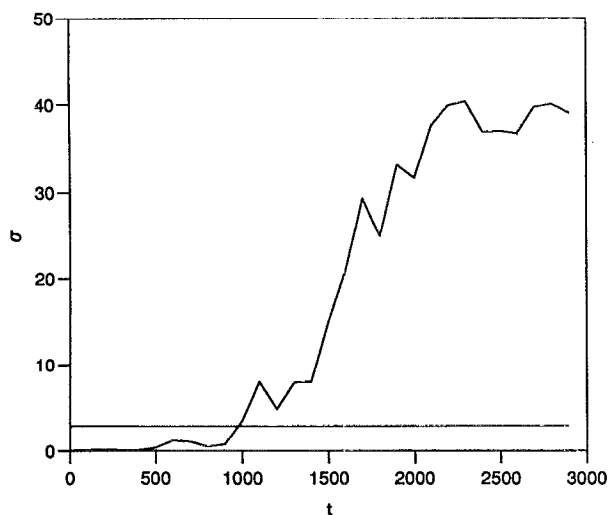


FIG. 8. Average size of the particle cloud,  $\sigma(t)$ , versus time, for the two particle distributions shown in Figs. 6 and 7. The size of the cloud is constant over all times for the particles in the regular island (constant horizontal line). Conversely, at small times  $\sigma_1(t)$  is exponentially growing for the particle cloud in the chaotic sea (upper curve). At large times, the chaotically moving particles fill the (Lagrangian) chaotic region, and  $\sigma(t)$  saturates to the size of the allowed domain.

$\lambda_L > 0$ , nearby particles undergo exponential divergence, and the cloud is rapidly stripped and dispersed, even in the presence of a regular (e.g., time periodic) Eulerian field.

To illustrate the above behaviors, in Figs. 6 and 7 we show the evolution of a particle cloud in the four-vortex field, for two different initial positions and sizes of the passive cloud. In Fig. 6 we report the case of a square cloud with size 2.0, centered on one of the four vortices (a square cloud has been used just for computational simplicity). The different clouds shown in the figure correspond to different instants of time. The size of the cloud does not increase and the particles remain trapped close to the vortex; no particle is ejected from the regular island surrounding the vortex. Figure 7 reports the case of a smaller cloud, with size 0.2, placed in the background chaotic region between the vortices; again, the four clouds refer to four instants of time. In this case, the cloud is stirred and folded with the usual mechanisms observed in chaotic systems, and the particles are dispersed. Clearly, the behavior of the cloud is very different in the two cases; this difference is accounted for by the values of the Lagrangian Lyapunov exponent.

As a further illustration, in Fig. 8 we show the increase of the average size of the advected cloud  $\sigma(t)$  as a function of time,

$$\sigma^2(t) = \frac{1}{M} \sum_{j=1}^M \{ [x^{(j)}(t) - x_B(t)]^2 + [y^{(j)}(t) - y_B(t)]^2 \}, \quad (13)$$

where  $[x^{(j)}(t), y^{(j)}(t)]$  is the position of the  $j$ th particle and  $[x_B(t), y_B(t)]$  is the position of the center of mass of the cloud. At small times,  $\sigma$  undergoes exponential growth for the chaotic case, roughly one has  $\sigma^2(t) \approx \exp(2\lambda_L t)$ . At large times, the particles of the chaotic cloud are dispersed in the

entire allowed domain, and the variance saturates at the size of the domain. Figures 9(a)–9(d) report the distribution of 10 000 passive particles at different times, until saturation in  $\sigma$  is reached. The initial condition on the cloud is the same as in Fig. 7.

From Fig. 9, a few observations may be drawn. First, we note that the passive particles remain inside an almost circular region, centered on the point  $\mathbf{x}_c = (\sum_{i=1}^4 \Gamma_i \mathbf{x}_i) / (\sum_{i=1}^4 \Gamma_i)$  (which does not move due to conservation laws). Passive particles that start inside this region, and far enough from each vortex, behave chaotically. Inside the chaotic domain, the particle distribution shown in Fig. 9 is not, however, completely uniform. In fact, from the figure, one may see that the four vortices are surrounded by four “holes” in the particle distribution. This result confirms the existence of a strong barrier separating the regular dynamics in proximity of each vortex, and the chaotic dynamics in the sea between the vortices (but inside the external separatrix). Particles seeded close to a vortex are trapped inside the regular islands, while particles seeded outside cannot penetrate the vortex islands. Each vortex carries the regular island with itself (from the point of view of passive particle advection), even though it may perform an irregular and chaotic trajectory on the plane.

#### IV. ADVECTION IN 2-D TURBULENCE

In previous sections, we have shown that the behavior of passive particles in point vortex systems depends upon the particle distance from the vortex centers. The presence of irregular trajectories is due to the time-dependent nature of the Hamiltonian system (2), which, in general, also leads to chaotic behavior for simple Eulerian flows. One may wonder whether a much more complex Eulerian flow, such as 2-D turbulence, may give the same scenario for particle advection: i.e., regular trajectories close to the vortices and chaotic behavior between the vortices. In this section, we show that this is indeed the case and that the chaotic nature of the trajectories of advected particles is not strictly determined by the complex time evolution of the turbulent flow.

To this end, here we study the Lagrangian dynamics by integrating the equations of motion (2) of an ensemble of passively advected particles in the streamfunction obtained by numerically integrating the forced-dissipative Navier–Stokes equations in two dimensions. The Eulerian equations of motion are given by

$$\frac{\partial \omega}{\partial t} + J(\omega, \psi) = F + D, \quad (14)$$

where  $\psi$  is the streamfunction,  $\omega = \Delta \psi$  is the vorticity, and  $J$  is the two-dimensional Jacobian. The velocity vector is given by  $\mathbf{u} = (\partial \psi / \partial y, -\partial \psi / \partial x)$ . The terms  $F$  and  $D$  indicate forcing and dissipation, respectively. In the case of two-dimensional turbulent flows, it is well known the presence of an *inverse* energy cascade from small to large scales and of a direct enstrophy cascade, enstrophy being the squared vorticity. Dissipation is thus required both at small scales (in order

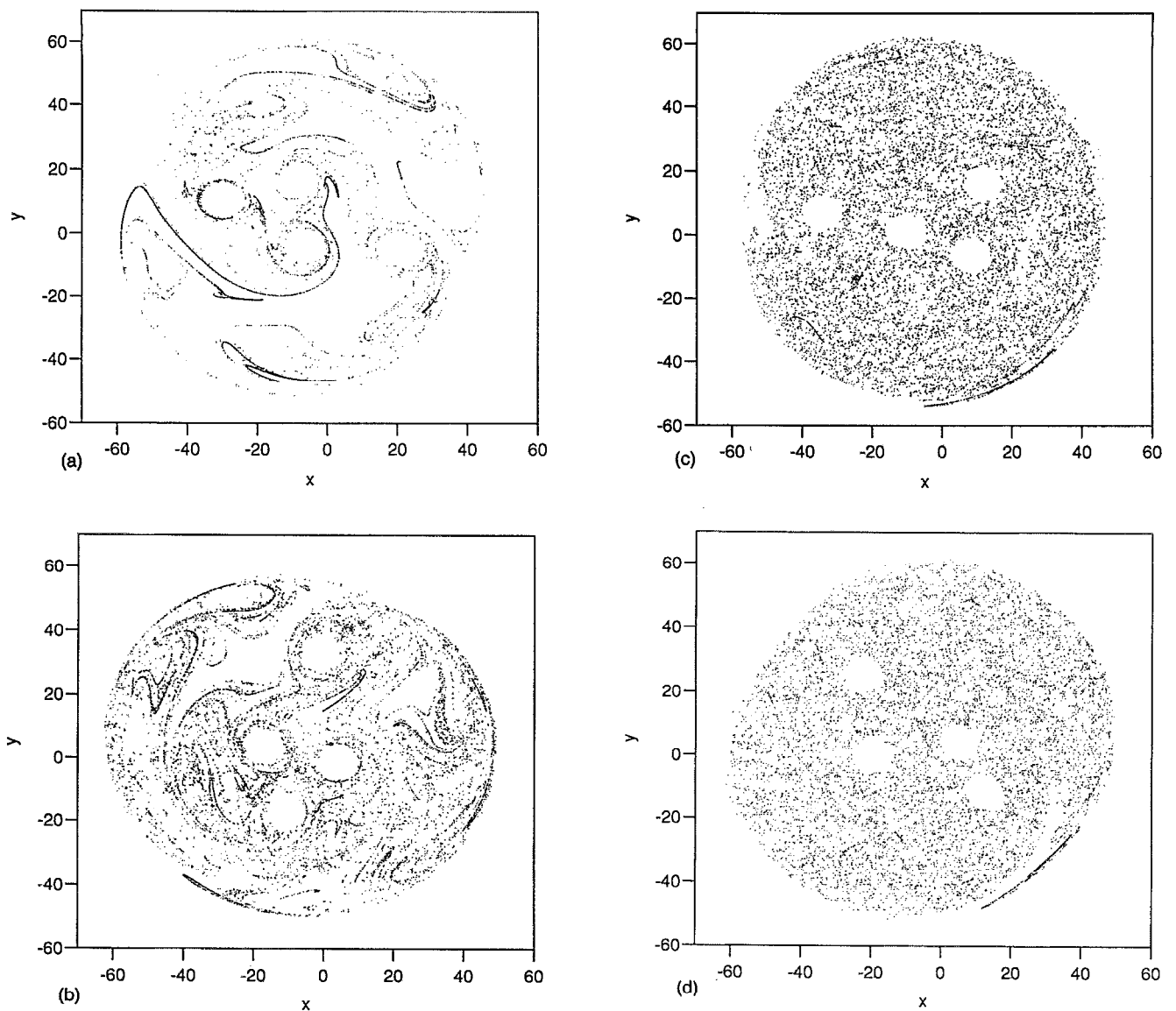


FIG. 9. Positions of 10 000 Lagrangian particles at four late times. Panels (a)–(d) refer to the times  $t=2000$ , 2500, 3500, and 4000 natural time units. The Lagrangian particles tend to fill the entire chaotic region among the vortices, while not entering the regular regions surrounding the four moving vortices. Each “hole” in the particle distribution is centered on one of the four point vortices.

to dissipate enstrophy and avoid ultraviolet divergences) and at large scales, in order to dissipate the energy piled up at these scales by the inverse cascade.

A typical vorticity field of a two-dimensional turbulent flow is characterized by the presence of long-lived coherent vortices immersed in a low-energy background turbulent field, see e.g., Refs. 26–35. While the latter is reasonably well described by a classic Batchelor–Kraichnan statistical approach,<sup>36–38</sup> the coherent vortices behave as individual entities, which cannot be treated with standard perturbative approaches. In fact, the dynamics of the coherent vortices in freely decaying 2-D turbulence has been compared with the motion of point vortex systems, finding interesting similarities.<sup>31–33</sup> In forced turbulence, the vortices interact among themselves and with the background turbulent field, which is much more active than in the case of freely decaying turbulence. Additionally, while in decaying turbulence

the vortex sizes may assume a large spectrum of values, in forced turbulence all vortices have a similar size, which is determined by the value of the forcing wave number.

Given the basic distinction between coherent vortices and background turbulence, we now want to explore the differences between the Lagrangian dynamics in the interior of coherent structures and in the background turbulence. Details on the Eulerian numerical simulations discussed here may be found in Refs. 26 and 27. To obtain the velocity field, the barotropic two-dimensional vorticity equation (14) has been integrated on a doubly periodic square lattice  $(2\pi, 2\pi)$  by a pseudospectral approximation. The forcing is defined by keeping constant the amplitude of a selected zonal mode ( $k_z$ ); the dissipation is provided by both a hyperviscosity at large wave numbers and by an Eckman-type dissipation at small wave numbers. These types of forcing and dissipation have been widely discussed and employed in past numerical

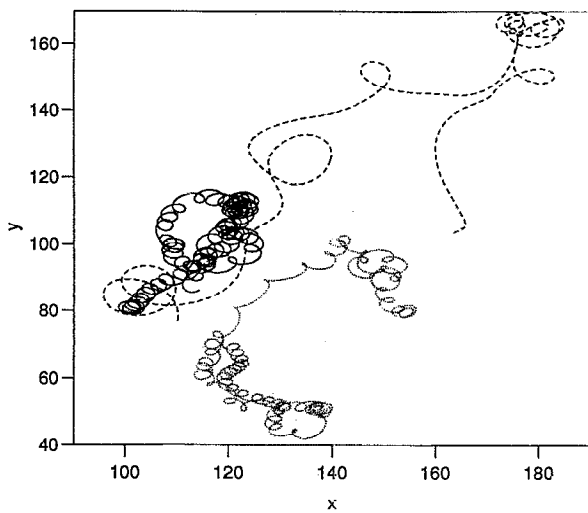


FIG. 10. Trajectories of three example Lagrangian particles in 2-D turbulence. The solid line refers to a particle that is trapped into a coherent structure, the dashed line refers to a particle moving in the turbulent field among the vortices, and the dotted line indicates the trajectory of a particle that is ejected from a coherent vortex.

simulations of 2-D turbulence.<sup>28-30,35</sup> Because of the intrinsic discrete nature of the Eulerian simulations, a proper interpolation scheme is needed in order to integrate the particle trajectories [Eq. (2)] and to compute the associated Lagrangian Lyapunov exponent  $\lambda_L$  [Eqs. (7) and (8)]. The scheme adopted herein is based on a third-order spline interpolation and on a second-order Runge-Kutta time integration.<sup>27,39,40</sup> Several different numerical experiments have been performed in order to obtain good confidence on the independence of the computed values on the resolution and on the interpolation scheme. Further details on the Lagrangian integrations may be found in Refs. 39 and 40.

In the present numerical experiments, the resolution of the Eulerian field has been chosen to be  $128^2$  grid points, and the forcing wave number has been chosen to be  $k_l=10$ , in order to obtain a vorticity field dominated by large coherent structures; see e.g., Refs. 26, 27, and 40 for graphic illustrations of these fields. The nondimensional kinetic energy of the field is  $E_{\text{mean}}=53.3$ , and the nondimensional Eulerian enstrophy is  $Z_{\text{mean}}=2600$ . The mean nondimensional Eulerian time scale is  $T_E=0.14$  and the mean nondimensional Lagrangian time scale is  $T_L=0.035$ . To obtain the particle trajectories and the Lyapunov exponents, we integrate an already stabilized Eulerian flow for a 20 000 time step (where the time step is  $\delta t=10^{-4}$ ), together with the motion of an ensemble of particles initially seeded in proximity of three different vortices. For simplicity, here we discuss only the results obtained for the simulations with resolution  $128^2$ . We have repeated the numerical experiments considered here with a higher resolution ( $256^2$ ) and with different forcing wave numbers, obtaining the same types of behavior. To explore the Lagrangian behavior, we have conducted a specific numerical experiment, where we have analyzed the trajectories of 1500 particles seeded in the Eulerian flow.

Figure 10 shows three trajectories that represent the typi-

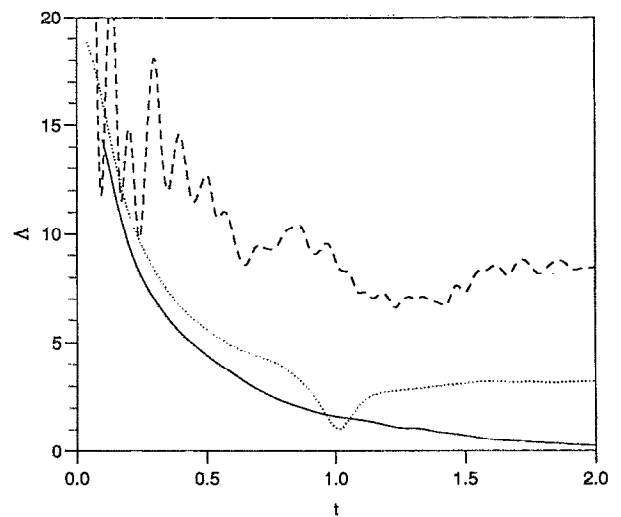


FIG. 11. Values of the quantity  $\Lambda_L(t)$  versus time for the three typical particle trajectories in 2-D turbulence shown in Fig. 10. Here  $\Lambda_L(t)$  converges to zero for the particle in the vortex (solid curve); it saturates to a constant positive value for a particle moving in the background and in the circulation cells (dashed curve). For the particle that is ejected from a vortex,  $\lambda_L(t)$  first decreases as  $t^{-1}$  and then saturates to a constant value after ejection (dotted curve).

cal behaviors observed for the advected particles (for an interesting comparison with real geophysical flows, see, e.g., Fig. 1 of Ref. 41). Passive particles initially seeded in the deep interior of a vortex core (solid curve) undergo a regular oscillatory motion around the center of the moving vortex, as already observed for the simple point vortex system discussed in the previous sections. Particles starting in the background turbulence (dashed curve) undergo a complex and unpredictable motion, again in analogy with the results obtained in the case of the point vortices. Usually, particles seeded into the background field do not enter the cores of existing vortices, which display a strong impermeability to inward particle fluxes.<sup>26,40</sup> On the other hand, particles seeded inside coherent structures but close to the outer boundary of the vortex may be ejected from it; this is the case of the dotted curve in Fig. 10. Usually, particle ejection from the coherent structures is associated with filamentation during close vortex interactions; an analogous behavior may also be observed for closely interacting point vortices, and will be discussed in a forthcoming paper.

To properly characterize the nature of the particle motions in 2-D turbulence, we have computed the Lagrangian Lyapunov exponents for a particle residing inside a coherent structure for the entire simulation time, for a particle moving in the background and for a particle that is ejected from the vortex during the simulation time. Figure 11 reports the quantity  $\Lambda_L(t)$  given by (8) for the above three passive particle trajectories. This quantity converges to zero for the particle inside coherent structures, indicating a null value of  $\lambda_L$  and a regular Lagrangian motion of the advected particles inside the vortices. This result is completely consistent with the behavior of passive particles in point vortex systems, and it indicates the absence of Lagrangian chaos inside the coherent structures of 2-D turbulence. In our opinion, this re-



sult is interesting, since it indicates the existence of islands of regular Lagrangian motion, even in turbulent Eulerian flows.

By contrast,  $\Lambda_L(t)$  converges toward a finite, positive value for the particle moving in the background turbulent field (dashed curve). This indicates the chaotic nature of particle motion in this region of 2-D turbulent flows; this result is a clear indication that chaotic advection may play a relevant role also for particle dispersion in turbulent Eulerian flows. Note the similarity between the results found here for the case of 2-D turbulence and those obtained for simple point vortex models, a fact that suggests that the detailed structure and time evolution of the Eulerian flow is not crucial for determining the Lagrangian dynamics of the advected particles. In fact, the Lagrangian dynamics seem to be mainly determined by the overall separatrix structure of the Eulerian field (e.g., the position of the hyperbolic points).

For the particles that are ejected from the vortices, the quantity  $\Lambda_L(t)$  decreases toward zero as long as the particles remain in the vortices. After ejection, the particles move in the background, and their behavior is indistinguishable from that of particles initially seeded outside the vortices. The value of  $\Lambda_L(t)$  may undergo an abrupt change when the particle is ejected from the vortex. Later on,  $\Lambda_L(t)$  converges to a finite positive value, confirming the chaotic nature of the particle motion in the background field.

## V. SUMMARY AND CONCLUSIONS

The existence of unpredictable, chaotic trajectories of passively advected particles in simple laminar 2-D flows with a time-periodic streamfunction is a well-known result, which has been given the name of *chaotic advection*. Here we have considered the case of complex, non-time-periodic Eulerian flows (namely, point vortex systems and forced-dissipative 2-D turbulence), and we have studied the chaotic or regular nature of particle trajectories.

In the case of point vortex systems, we have shown that the chaotic or regular nature of Lagrangian particle motions does not strictly depend on the detailed properties of the Eulerian advecting flow (being insensitive even to its regular or chaotic nature); it rather depends only on purely Lagrangian quantities, such as the particle distance from the vortex centers. In particular, we have shown that around each point vortex there is a regular island of particle trapping; here the passive particle dynamics is characterized by a null Lagrangian Lyapunov exponent. Sufficiently far from the vortices, the passive particles move chaotically and the Lagrangian Lyapunov exponent is positive.

The above results indicate that regular regions of Lagrangian advection may exist, even in complex Eulerian flows. This observation was already advanced in Ref. 14 in the case of the Lorenz model, which is, however, a somewhat pathological case from the point of view of Lagrangian chaos, due to the form of the velocity field. The results discussed here on point vortex dynamics confirm the general existence of regular islands in complex, chaotic Eulerian flows and underline the difficulty of finding strict relationships between the Eulerian and Lagrangian description of the same fluid flow.

In the case of 2-D turbulence, the analysis of 1500 particle trajectories in a forced-dissipative,  $128^2$  resolution numerical integration of the Navier–Stokes equations has revealed an analogous scenario, with a regular Lagrangian motion inside the coherent structures and chaotic advection of passive particles in the background turbulent field among the vortices. Again, we stress the fact that regular regions of Lagrangian motion may exist, even in turbulent Eulerian flows.

As a general conclusion, we note that the results reported here indicate that the detailed structure of the advecting Eulerian field seems to be of limited importance in determining the behavior of the passive tracers. In particular, the similarity of the results between point vortex systems and 2-D turbulence suggest that the exact time evolution of the velocity field is not crucial for the particle dispersion properties, being sufficient a generic nonstationarity of the advecting field. In this sense, it is probably much more important the overall separatrix structure of the Eulerian field, namely the existence and the position of hyperbolic and elliptic points. In general, one may also conclude that the same presence or absence of an Eulerian turbulent dynamics seems not to be crucial from the point of view of particle dispersion properties.

## ACKNOWLEDGMENTS

We acknowledge support from the EEC, Contract No. CHRX-CT92-0001, “Two-dimensional turbulence, vortices and geophysical flows,” and from the “Groupement de Recherche CNRS-IFREMER, Mécanique des Fluides Géophysiques et Astrophysiques.” The numerical computations were performed under Contract No. 2946 of the “Centre de Calcul Vectoriel pour la Recherche.” We are grateful to Professor J. M. Ottino and to an anonymous referee for their careful reading of the manuscript and for useful suggestions.

- <sup>1</sup>A. S. Monin and A. M. Yaglom, *Statistical Fluid Mechanics* (MIT Press, Cambridge, MA, 1975), Vol. 2.
- <sup>2</sup>J. M. Ottino, *The Kinematic of Mixing: Stretching, Chaos and Transport* (Cambridge University Press, Cambridge, 1989).
- <sup>3</sup>J. M. Ottino, “Mixing, chaotic advection, and turbulence,” *Annu. Rev. Fluid Mech.* **22**, 207 (1990).
- <sup>4</sup>A. Crisanti, M. Falcioni, G. Paladin, and A. Vulpiani, “Lagrangian chaos: Transport, mixing and diffusion in fluids,” *Riv. Nuovo Cimento* **14**, 1 (1991).
- <sup>5</sup>S. Wiggins, *Chaotic Transport in Dynamical Systems* (Springer, New York, 1992).
- <sup>6</sup>H. Aref, “Stirring by chaotic advection,” *J. Fluid Mech.* **143**, 1 (1984).
- <sup>7</sup>T. H. Solomon and J. P. Gollub, “Chaotic particle transport in time-dependent Rayleigh–Benard convection,” *Phys. Rev. A* **38**, 6280 (1988).
- <sup>8</sup>J. B. Weiss and E. Knobloch, “Mass transport and mixing by modulated traveling waves,” *Phys. Rev. A* **40**, 2579 (1989).
- <sup>9</sup>V. Rom-Kedar, A. Leonard, and S. Wiggins, “An analytical study of transport, mixing and chaos in a unsteady vortical flow,” *J. Fluid Mech.* **214**, 347 (1990).
- <sup>10</sup>V. Rom-Kedar and S. Wiggins, “Transport in two-dimensional maps,” *Arch. Rat. Mech. Anal.* **109**, 239 (1990).
- <sup>11</sup>R. Camassa and S. Wiggins, “Chaotic advection in Rayleigh–Bénard flow,” *Phys. Rev. A* **43**, 774 (1991).
- <sup>12</sup>J. B. Weiss, “Transport and mixing in traveling waves,” *Phys. Fluids A* **3**, 1379 (1991).
- <sup>13</sup>D. del Castillo Negrete and P. J. Morrison, “Chaotic transport by Rossby waves in shear flow,” *Phys. Fluids A* **5**, 948 (1992).
- <sup>14</sup>M. Falcioni, G. Paladin, and A. Vulpiani, “Regular and chaotic motion of

- fluid particles in two-dimensional fluid," *J. Phys. A. Math. Gen.* **21**, 3451 (1988).
- <sup>15</sup>M. R. Maxey, "The motion of small spherical particles in a cellular flow field," *Phys. Fluids* **30**, 1915 (1987).
- <sup>16</sup>A. Crisanti, M. Falcioni, A. Provenzale, P. Tanga, and A. Vulpiani, "Dynamics of passively advected impurities in simple two-dimensional flow fields," *Phys. Fluids A* **4**, 1805 (1992).
- <sup>17</sup>A. J. Lichtenberg and M. A. Leibermann, *Regular and Stochastic Motions* (Springer-Verlag, Berlin, 1983).
- <sup>18</sup>E. Ott, *Chaos in Dynamical Systems* (Cambridge University Press, Cambridge, 1993).
- <sup>19</sup>G. R. Kirchhoff, *Vorlesungen uber Mathematische Physik* (Teubner, Leipzig, 1876).
- <sup>20</sup>H. Aref, "Integrable, chaotic, and turbulent vortex motion in two-dimensional flows," *Annu. Rev. Fluid Mech.* **15**, 345 (1983).
- <sup>21</sup>J. B. Weiss and J. C. McWilliams, "Nonergodicity of point vortices," *Phys. Fluids A* **3**, 835 (1991).
- <sup>22</sup>E. A. Novikov and Yu. B. Sedov, "Stochastic properties of a four-vortex system," *Sov. Phys. JETP* **48**, 440 (1978).
- <sup>23</sup>V. V. Meleshko, M. Yu. Konstantinov, A. A. Gurzhi, and T. P. Konovaljuk, "Advection of a vortex pair atmosphere in a velocity field of point vortices," *Phys. Fluids A* **4**, 2779 (1992).
- <sup>24</sup>G. Benettin, A. Giorgilli, L. Galgani, and J. M. Strelcyn, "Lyapunov characteristic exponents for smooth dynamical systems and for Hamiltonian systems; a method for computing all of them. Part 1: Theory, Part 2: Numerical applications," *Meccanica* **15**, 9, 21 (1980).
- <sup>25</sup>G. Benettin, L. Galgani, and J. M. Strelcyn, "Kolmogorov entropy and numerical experiments," *Phys. Rev. A* **14**, 2338 (1976).
- <sup>26</sup>A. Babiano, C. Basdevant, B. Legras, and R. Sadourny, "Vorticity and passive scalar dynamics in two-dimensional turbulence," *J. Fluid Mech.* **183**, 379 (1987).
- <sup>27</sup>A. Babiano, C. Basdevant, P. Le Roy, and R. Sadourny, "Relative dispersion in two-dimensional turbulence," *J. Fluid. Mech.* **214**, 535 (1990).
- <sup>28</sup>C. Basdevant, B. Legras, R. Sadourny, and M. Beland, "A study of barotropic model flows: Intermittency waves and predictability," *J. Atmos. Sci.* **38**, 2305 (1981).
- <sup>29</sup>J. C. McWilliams, "The emergence of isolated coherent vortices in turbulent flow," *J. Fluid Mech.* **146**, 21 (1984).
- <sup>30</sup>J. C. McWilliams, "The vortices of two-dimensional turbulence," *J. Fluid Mech.* **219**, 361 (1990).
- <sup>31</sup>R. Benzi, G. Paladin, S. Patarnello, P. Santangelo, and A. Vulpiani, "Intermittency and coherent structures in two-dimensional turbulence," *J. Phys. A* **19**, 3771 (1986).
- <sup>32</sup>R. Benzi, S. Patarnello, and P. Santangelo, "On the statistical properties of two-dimensional decaying turbulence," *Europhys. Lett.* **3**, 811 (1987).
- <sup>33</sup>R. Benzi, S. Patarnello, and P. Santangelo, "Self-similar coherent structures in two-dimensional decaying turbulence," *J. Phys. A* **21**, 1221 (1988).
- <sup>34</sup>M. Brachet, M. Meneguzzi, H. Politano, and P. Sulem, "The dynamics of freely decaying two-dimensional turbulence," *J. Fluid Mech.* **194**, 333 (1988).
- <sup>35</sup>B. Legras, P. Santangelo, and R. Benzi, "High-resolution numerical experiments for forced two-dimensional turbulence," *Europhys. Lett.* **5**, 37 (1988).
- <sup>36</sup>G. K. Batchelor, "Computation of the energy spectrum in homogeneous two-dimensional turbulence," *Phys. Fluids* **12**, 233 (1969).
- <sup>37</sup>R. H. Kraichnan, "Inertial ranges in two-dimensional turbulence," *Phys. Fluids* **10**, 1417 (1967).
- <sup>38</sup>R. H. Kraichnan and D. Montgomery, "Two-dimensional turbulence," *Rep. Prog. Phys.* **43**, 547 (1980).
- <sup>39</sup>N. Zouari and A. Babiano, "Experiences numeriques Lagrangiennes a partir de modeles euleriens," *Atmos. Ocean* **28**, 345 (1990).
- <sup>40</sup>D. Elhmaili, A. Provenzale, and A. Babiano, "Elementary topology of two-dimensional turbulence from a Lagrangian viewpoint and single-particle dispersion," *J. Fluid Mech.* **257**, 533 (1993).
- <sup>41</sup>P. L. Richardson, "Tracking ocean eddies," *Am. Sci.*, May-June (1993).